OPEN

Brown Tumors Belong to the Spectrum of *KRAS*-driven Neoplasms

Daniel Turek, MD, Simon Haefliger, MD,* Baptiste Ameline, PhD,* Ilaria Alborelli, PhD,† Byron Calgua, PhD,† Wolfgang Hartmann, MD,‡ Dorothee Harder, MD,§ Adrienne M. Flanagan, MD, PhD,‖¶ Fernanda Amary, MD, PhD,‖¶ and Daniel Baumhoer, MD**

Abstract: Brown tumors are rare and generally self-limiting mass lesions of bone occurring in the context of hyperparathyroidism. Although commonly regarded as endocrine-driven tumor-like lesions, we detected pathogenic hotspot *KRAS* mutations in 10/16 brown tumors (62%) with similar frequencies found in cases affecting the peripheral and axial skeleton. Pathogenic mutations in other driver genes of the RAS-MAPK pathway were not identified. Our findings suggest brown tumors to represent true neoplasms driven by the activation of the RAS-MAPK signaling pathway. The frequent regression of brown tumors after normalization of hyperparathyroidism points to a second hit mediated by endocrine stimulation to be required for tumor development. Our findings underline the pathogenic relation of brown tumors to nonossifying fibroma and giant cell granuloma of the jaws which both appear histologically similar to brown tumors and are also driven by RAS-MAPK signaling pathway activation.

Key Words: brown tumor, giant cell lesion, hyperparathyroidism, *KRAS* gene, RAS-MAPK pathway

(*Am J Surg Pathol* 2022;46:1577–1582)

Brown tumors (BTs) are rare lesions of bone occurring in the context of excessive parathyroid hormone (PTH) secretion due to dysregulated activation of the parathyroid gland.[1,2] The incidence of BT in hyperparathyroidism ranges between 1.5% and 3% in primary and secondary hyperparathyroidism, respectively. Since spontaneous regression after normalization of PTH levels is common and BT generally follow an indolent clinical course, they were traditionally assumed to represent reactive/tumor-like lesions.[3] On imaging, BT present as well-defined single or multiple osteolytic lesions, affecting the axial or peripheral skeleton.[4] Microscopically, they are characterized by mononuclear spindle cells arranged in lobular and storiform patterns showing intermingled osteoclast-like giant cells and hemosiderin-laden macrophages.[5] As their histologic appearance is virtually identical to giant cell granuloma of the jaws (GCG) and nonossifying fibroma (NOF) of bone, clinicopathologic correlation, especially regarding PTH levels, is mandatory to render the diagnosis.

The molecular pathogenesis of BT is incompletely understood. Recent advances in the field revealed that pathogenic driver mutations resulting in constitutive activation of the RAS-MAPK signaling pathway underlie GCG and NOF.[6,7] These findings changed the general perspective of both lesions which are now regarded true neoplasms. Similar to GCG and NOF, BT have historically been considered non-neoplastic and to arise as a direct consequence of hyperparathyroidism, mimicking osteitis fibrosa in the context of renal osteodystrophy.[8] Although PTH stimulation is clearly a prerequisite for tumor development, an additional genetic driver could explain why only a minority of patients with hyperparathyroidism develop BT.

Interestingly, hormone-mediated stimulation is also known to be involved in the development of bone tumors other than BT, for example, osteochondromas.[9] Indeed, during skeletal growth, human growth hormone (hGH)

From the *Bone Tumor Reference Centre, Institute of Medical Genetics and Pathology; †Institute of Medical Genetics and Pathology; §Department of Radiology, University Hospital Basel, University of Basel, Basel, Switzerland; ‡Division of Translational Pathology, Gerhard-Domagk-Institut of Pathology, University Hospital Münster, Münster, Germany; ‖Cellular and Molecular Pathology, Royal National Orthopaedic Hospital, Stanmore, Greater London; and ¶Research Department of Pathology, University College London, UCL Cancer Institute, London, UK.

D.T. and S.H. contributed equally.

Conflicts of Interest and Source of Funding: D.T., S.H., B.A., and D.B. were supported by the Swiss National Science Foundation, the Foundation of the Bone Tumor Reference Centre, the Gertrude von Meissner Stiftung and the Stiftung für krebskranke Kinder, Regio Basiliensis. A.M.F. is supported by the National Institute for Health Research, the Cancer Research UK University College London Experimental Cancer Medicine Centre, the RNOH Research and Development Department and the RNOH Biobank Team and the Tom Prince Trust. The authors have disclosed that they have no significant relationships with, or financial interest in, any commercial companies pertaining to this article.

Correspondence: Daniel Baumhoer, MD Bone Tumour Reference Centre, Institute of Medical Genetics and Pathology, University Hospital Basel, University of Basel, Schoenbeinstrasse 40, 4031 Basel, Switzerland (e-mail: daniel.baumhoer@usb.ch).

Supplemental Digital Content is available for this article. Direct URL citations appear in the printed text and are provided in the HTML and PDF versions of this article on the journal's website, www.ajsp.com.

has been shown to stimulate osteochondroma development and progression by stimulating insulin-like growth factor 1 (IGF1) expression, inducing the recruitment and stimulation of adaptive proteins that trigger RAS-MAPK signaling.[9] Whereas mutations in the *EXT1*/*EXT2* gene have been shown to genetically underlie osteochondroma development, the hormonal influence appears to play an important role for the commonly observed spontaneous growth arrest following skeletal maturation, which coincides with decreased level of hGH and IGF1. A similar mechanism might underlie NOF (also typically arising during skeletal growth) which, in contrast to osteochondroma, generally regress spontaneously and can completely dissolve.[9] It can therefore be hypothesized that in these self-limiting tumors an endocrine stimulus might induce proliferation of cells carrying pathogenic driver mutations and thus function as a "second hit."

A recent study by Guimaraes et al[10] demonstrated activating mutations in *KRAS* in about 50% of gnathic BT. Based on an index case of a 58-year-old male with known primary hyperparathyroidism presenting to our hospital with a pathologic fracture of the left humerus and subsequent diagnosis of a BT, we screened a series of BT affecting the axial and peripheral skeleton for underlying mutations involving the RAS-MAPK signaling pathway.

MATERIALS AND METHODS

Tumor Samples

Twenty-six formalin-fixed paraffin-embedded (FFPE) tissue samples from patients with BT were included in the study, comprising 20 cases from the Bone Tumor Reference Center in Basel (CH) and 6 cases from the Royal National Orthopaedic Hospital in Stanmore (UK). The diagnosis was confirmed by experienced pathologists with a particular expertise in bone and soft tissue pathology. The study was approved at the University Hospital Basel, following the approval of the ethical committee for mutational analysis of samples ("Ethikkommission beider Basel" ref. 274/12). The Royal National Orthopaedic Hospital Biobank is approved by the National Research Ethics Committee of the Health Research Committee (reference: Integrated Research Application System [IRAS] project identifier: 272816). This study was approved by the National Research Ethics Committee approved UCL/UCLH Biobank Ethics Committee (project no: EC17.14).

Sequencing

Gene panel sequencing (Ampliseq Solid Tumor DNA—Colon and Lung V2 Panel) and Sanger sequencing were carried out following routine protocols (for details, see Supplement, Supplemental Digital Content 1, http://links.lww.com/PAS/B426). Variant calling was performed on Ion Reporter Analysis Software. Polymorphisms were filtered against UCSC common SNP, ExAC, 1000 Genomes and 5000 Exomes databases. Detected sequence variants were evaluated for their pathogenicity based on previous literature, databases (COSMIC, ClinVar) and classified as pathogenic, variant of unknown significance, and benign.

RESULTS

Clinical Features

The average age at diagnosis was 49 years (range: 18 to 82 y, median: 42 y), our study included 14 males and 12 females. The majority of tumors (68%) were found in the peripheral skeleton, while a minority was located in the axial skeleton (32%). In most patients, BT occurred in the context of secondary hyperparathyroidism due to renal insufficiency (79%), the remaining patients had a history of primary hyperparathyroidism (21%). Imaging was available in 6 cases and showed predominantly lytic lesions with an average size of 3 cm (range: 2 to 5 cm), located in the trunk, skull, and peripheral skeleton (Fig. 1). One patient presented with multiple lesions in both hands; however, the exact number of tumors could not be determined due to missing clinical and radiologic information. According to the clinical records, the other patients showed monostotic involvement only. Full-body imaging of the skeleton was not available for any of the patients. Curettage was performed in 8 cases (50%), and biopsy or resection in 6 and 2 cases, respectively (38%, 12%). Follow-up data were available in 6 cases, with an

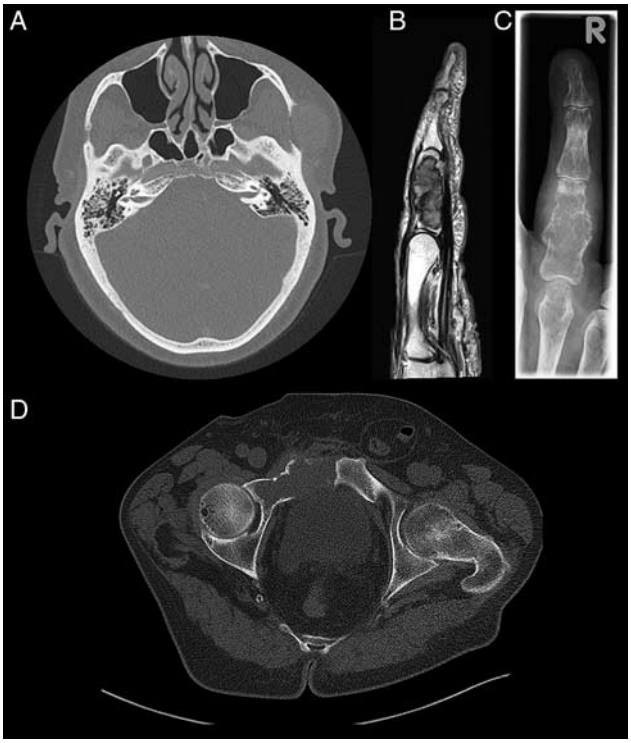

FIGURE 1. Representative imaging findings of BTs. A, Axial computed tomography scan of the skull shows a lytic lesion of the left zygomatic arch with a distinct extraosseous component. T2-weighted sagittal magnetic resonance imaging (B) and corresponding x-ray (dorsoplantar view; C) of the digit of the right hand show a geographic expansile lytic lesion with intermediate signal intensity of the middle phalanx. D, Axial computed tomography scan of the pelvis shows a purely lytic lesion of the right superior pubic ramus with cortical breakthrough.

TABLE 1. Summary of the Clinical and Pathologic Features

Patient #	Age at Diagnosis (y)	Sex	Tumor Localization	Radiology	Type of Hyperparathyreoidism	FU Time (mo)	KRAS	FGFR1	TRPV4	Procedure	Tumor Content (%)	Tumor Size (cm)
1	35	F	Right maxilla	NA	Secondary	NA	G12D (AF = 0.27)	WT	WT	Curettage	80	NA
2	70	M	Left humerus	NA	Secondary	NA	A146P (AF = 0.15)	WT	WT	Curettage	80	NA
3	33	F	Right mandible	X-ray	Secondary	5	A146T (AF = 0.02)	WT	WT	Resection	80	4
4	68	M	Right zygomatic arch	CT	Secondary	NA	WT	WT	WT	Curettage	80	4
5	77	M	Right upper pubic ramus	CT	Secondary	NA	A146V (AF = 0.15)	WT	WT	Biopsy	70	5
6	73	M	Right hand, distal phalanx III	X-ray	NA	NA	WT	WT	WT	Curettage	90	2
7	41	M	NA	NA	Secondary	36	K117R (AF = 0.26)	WT	WT	Biopsy	80	NA
8	65	M	NA	NA	Secondary	3	A146T (AF = 0.21)	WT	WT	Biopsy	80	NA
9	28	F	Bilateral hands	NA	NA	NA	WT	WT	WT	Resection	80	NA
10	43	F	Right femur	NA	Primary	NA	WT	WT	WT	Curettage	20	NA
11	41	M	Os sacrum	NA	Secondary	NA	G12D (AF = 0.24)	WT	WT	Biopsy	90	NA
12	76	F	NA	NA	Secondary	1	G13C (AF = 0.16)	WT	WT	Biopsy	20	NA
13	58	M	Left humerus, capitulum	X-ray, MRI	Primary	NA	Q22K (AF = 0.21)	WT	WT	Curettage	80	2
14	82	M	Right hand, proximal Phalanx IV	X-ray, MRI	Secondary	NA	A146V (AF = 0.24)	WT	WT	Curettage	90	2
15	18	F	Left tibia, proximal	NA	Primary	13	WT	WT	WT	Curettage	50	NA
16	63	M	Left os ilium	NA	Secondary	38	WT	WT	WT	Biopsy	50	NA

Table with summary of the clinical data of all cases (n = 16), including sex, age at diagnosis, localization, radiology, type of hyperparathyroidism, follow-up, and mutational status of *KRAS*, *FGFR1*, and *TRPV4*.

CT indicates computed tomography; F, female; FU, follow-up; M, male; MRI, magnetic resonance imaging; NA, not available; WT, wild-type.

average follow-up time of 9 months (range: 1 to 38 mo). In 2 cases, tumor regression was documented following normalization of PTH levels. All clinicopathologic data are summarized in Table 1.

Histologically, all tumors had a similar appearance consisting of monomorphic spindle cells arranged in a patternless and partly storiform pattern and intermingled multinucleated giant cells. The osteoclast-like giant cells were small compared with those seen in giant cell tumor of bone, evenly distributed and contained less than ten nuclei per tissue section on average. Mitotic activity was low and there were no atypical mitotic figures; significant cellular atypia and/or tumor necrosis was absent. Hemosiderin-laden macrophages, considered responsible for the brown color of BT, were present to varying degrees as were extravasated erythrocytes. Most tumors showed fibrous septae with reactive new bone formation that incompletely subdivided the tumor into lobules. Adjacent preexisting bone was not present in the majority of cases and morphologic features of mineral and bone disorder in the context of chronic kidney disease was not observed. A representative selection of the histologic appearance is shown in Figure 2. The tumor cell content, represented by the mononuclear cells of the specimens, was 70% on average (range: 20% to 90%).

Sequencing Data

Sequencing was successfully performed in 16/26 tissue samples. For the remaining cases, insufficient DNA quality prevented molecular analyses. The analyses revealed pathogenic hotspot mutations in the *KRAS* gene in 10/16 tumors (62%). The most common alterations were p.A146P/T/V and p.G12D mutations, which account for 70% of all *KRAS* mutations. Other activating mutations included p.G13C (n = 1), p.K117R (n = 1), p.Q22K (n = 1). The allelic frequencies (AF) ranged from 0.02 to 0.27 (mean: 0.19, SD: 0.07). *KRAS* mutations were found in BT in both the axial (n = 4) and the peripheral (n = 3) skeleton. In the 3 remaining cases with *KRAS* mutation, the anatomic site was not available. *FGFR1* and *TRPV4* mutations previously detected in GCG and NOF were not identified. In 10/26 cases, sequencing analyses failed due to insufficient tissue and/or DNA preservation. It would have

been valuable to compare the genetic profile of distinct tumors from the same patient but unfortunately, tissue samples for performing such a comparison was not available. All sequencing data are summarized in Table 1 as well as in Figures 3 and 4.

DISCUSSION

In this study, we performed targeted sequencing in a cohort of patients with BT and found pathogenic *KRAS* mutations in almost two third of the cases.

The RAS-MAPK pathway is a highly conserved signaling pathway involved in a wide range of cellular processes, including cell proliferation and survival.[11] Mutations in the genes involved are present in around 30% of malignant neoplasms and activating *KRAS* mutations have been described in a broad range of tumors, including colorectal and non–small cell lung carcinoma.[12,13] Interestingly, the same mutations have increasingly been identified also in non-neoplastic conditions such as endometriosis, arteriovenous malformations and even histologically normal endometrium, indicating that the sole presence of a driver mutation is not sufficient to cause cancer.[14–16] Indeed, inverse correlations have been observed for *BRAF* mutations: for instance, 80% of benign melanocytic nevi harbor this mutation, whereas it is present in only 40% of malignant melanomas.[17] The context in which the RAS-MAPK signaling pathway is activated, including the cell affected and the interaction with the microenvironment among others, therefore seems essential for its pathogenic impact.[9] Our data in BT along with similar findings in gnathic tumors described by Guimaraes et al[10] constitute strong evidence that BT should be considered *KRAS*-driven neoplasms and add another lesion to the broad family of tumors that are caused, or at least influenced, by constitutive RAS-MAPK signaling activation. Furthermore, our data suggest that the site of origin of BT does not impact mutational status because peripheral and axial BT show identical *KRAS* mutation rates.

Long-standing hyperparathyroidism is an increasingly rare condition in patients with access to high standards of care. It is, therefore, difficult to assemble large sets of these rare lesions that uniformly follow a benign clinical course.[2] In addition, only 2% of patients with hyperparathyroidism develop BT. Thus, an elevated serum PTH level appears to be a mandatory yet not sufficient factor for the development of BT. In contrast, BT tend to regress

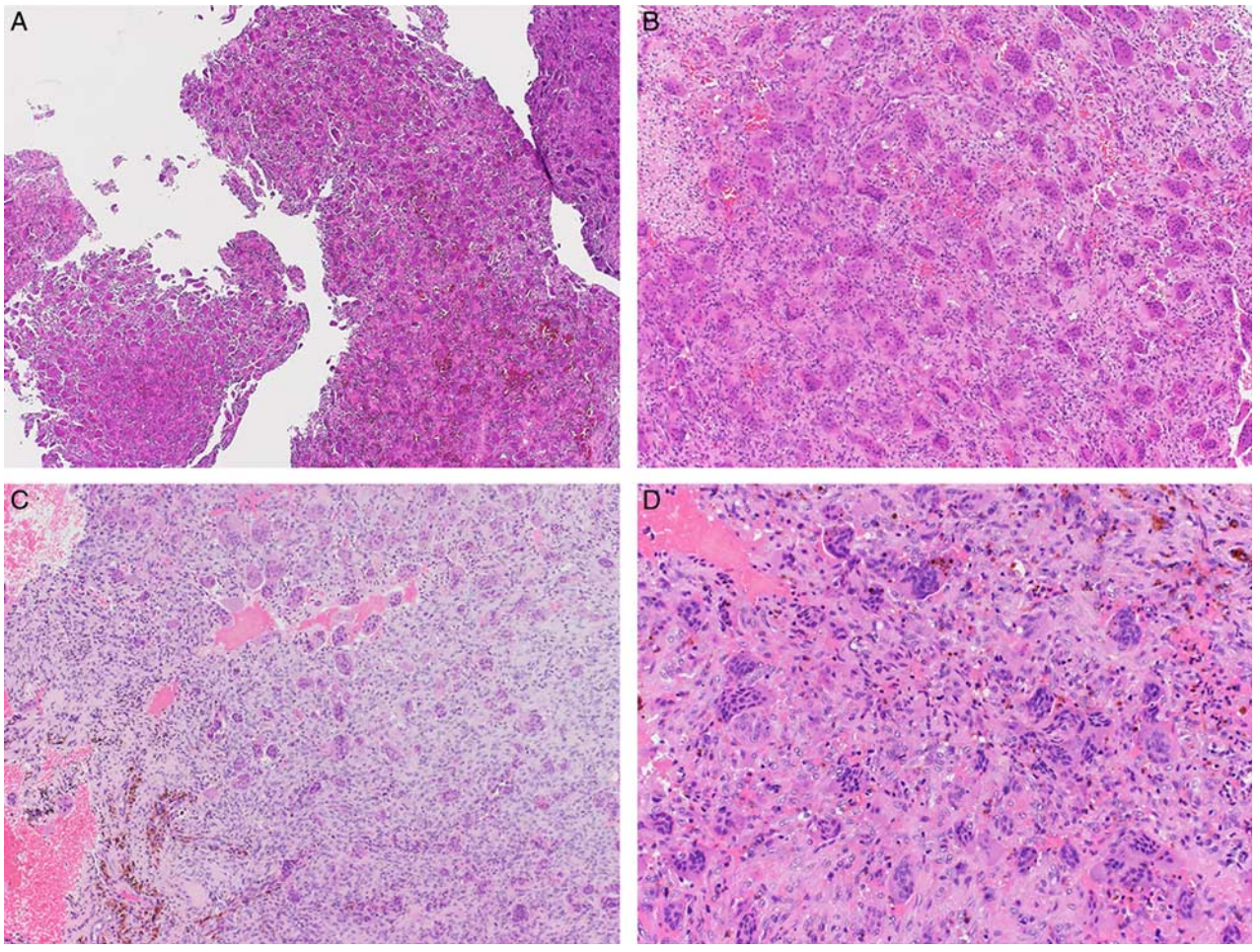

FIGURE 2. Representative histology of BTs. A–D, Typical morphology of BTs with osteoclast-like giant cells embedded in a fibrous stroma containing hemosiderin deposits and extravasated erythrocytes. Cellular atypia or mitosis are absent.

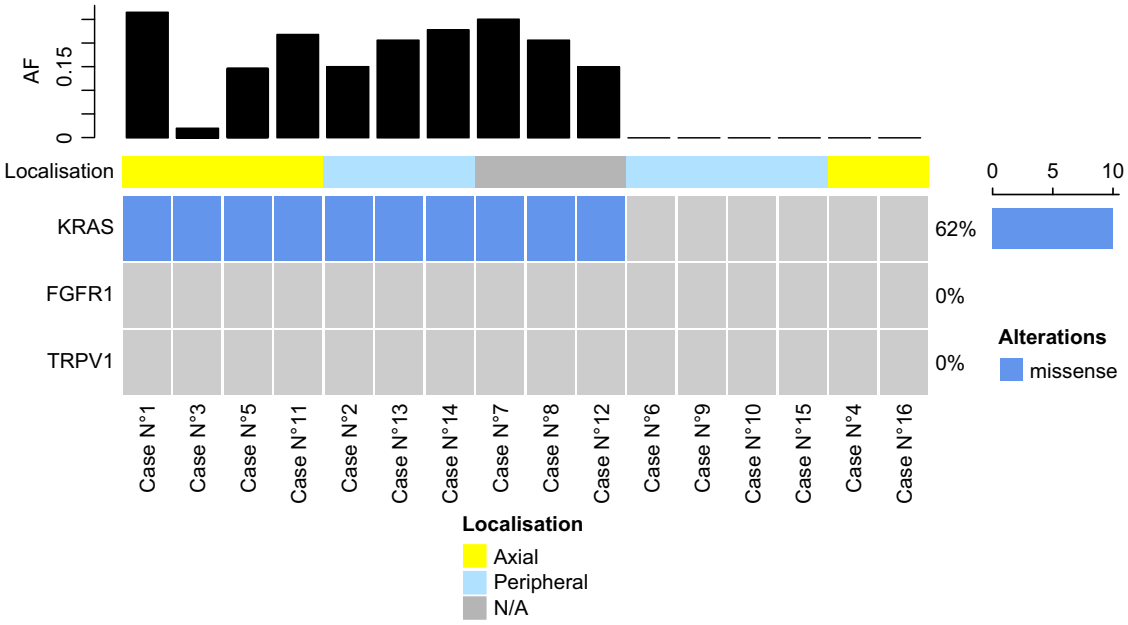

FIGURE 3. Overview of clinical and molecular features. OncoPrint with each column representing a patient with additional information about the tumor localization and each row representing specific genes. NA indicates not available.

spontaneously following normalization of PTH secretion. In this regard, BT share similarities with NOF as both lesions are usually self-limited and seem to be influenced by endocrine stimulation.[9] In NOF, increased estrogen levels during puberty have been hypothesized to interfere with RAS-MAPK overactivation and to terminate tumor growth. Similar observations have been made also in osteochondromas, which cease growing after skeletal maturation, most probably due to a decrease in hGH and IGF1 levels.[9] In this regard, endometriosis, another hormonal-dependent lesion with underlying driver mutations, including *KRAS* mutations, among others, shares similarities with BT. Indeed, in both lesions a hormonal stimulus seems to act as a "second hit" and unlock the growth potential of the mutated cells (Fig. 5). Such hormonal triggers might serve as the underlying mechanism also in other self-limiting tumors. In addition, since neoplasms might best be defined as a cellular proliferation with an underlying and driving genetic or epigenetic alteration, lesions traditionally considered non-neoplastic such as endometriosis might undergo a change in perception. Fibrous dysplasia (FD), a classic example of a benign tumor-like lesion, has also been revised as neoplastic disease according to the current WHO classification.[19]

The cause of *KRAS* mutations in BT is unclear, but as mentioned above, *KRAS* mutations have also been found in normal and non-neoplastic, tumor-like tissues as well as being associated with age and smoking.[20] In 6/16 of our sequenced cases, neither *KRAS*, nor *FGFR1* or *TRPV4* mutations were found. In these, an alternative, non-mutational based activation of the RAS-MAPK might be speculated. In the mutated cases, we noticed a low AF of *KRAS* mutation despite high tumor cell content in the specimens. This might be explained by the fact that the neoplastic cells in BT do not represent the predominant cell population or that only a subpopulation of cells harbors the mutation. FD, a fibro-osseous lesion of bone caused by mosaic *GNAS* mutations, behaves in a similar manner to BT and NOF. Indeed, as the skeleton matures, FD lesions often (but not always) cease to grow and mature / develop regressive changes. As the underlying mechanism of this phenomenon, progressive apoptosis of

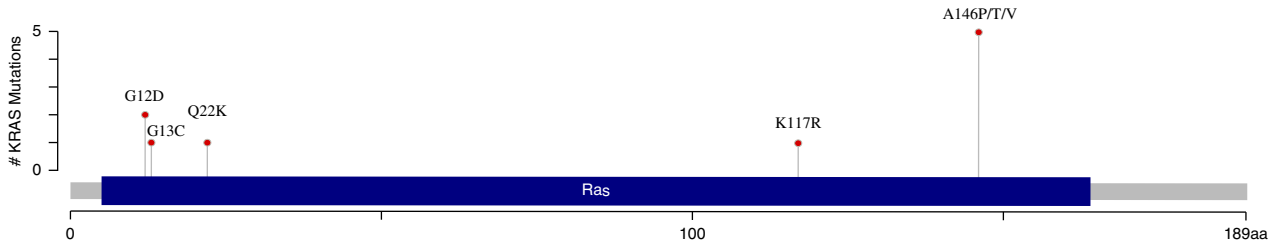

FIGURE 4. Lolliplot of the gene *KRAS*. Illustrative representation of the gene *KRAS* with mapping of the mutations observed along the gene.

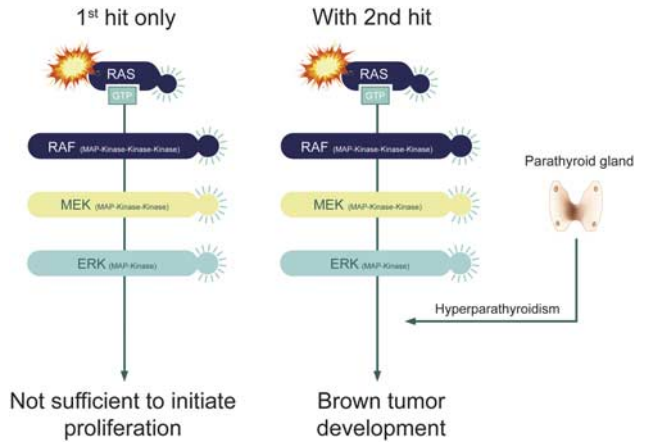

FIGURE 5. Schematic illustration of the proposed model for the pathogenesis of BTs. Sequential, 2-hit model leading to the development of BTs with the first hit being an activation of the MAPK pathway—insufficient on its own for neoplastic growth—followed by a second hit, a hormonal stimulus (elevation of PTH) leading to oncogenic growth. Illustration modified from Molecular Biology of the Cell by Alberts et al.[18] Adaptations are themselves works protected by copyright. So in order to publish this adaptation, authorization must be obtained both from the owner of the copyright in the original work and from the owner of copyright in the translation or adaptation.

the mutant cells has been proposed which is also reflected by a decrease in AF of the *GNAS* mutation over time that can ultimately drop below the detection threshold of the individual analysis method used.[21] Similarly and depending on the degree of stimulation by PTH, the number of KRAS mutated cells in BT could diminish over time, making the mutation increasingly difficult to detect.

To the best of our knowledge, our study is the first to describe pathogenic hotspot *KRAS* mutations in BT of the peripheral and axial skeleton, suggesting that these tumors are indeed true neoplasms that require both a mutation in the *KRAS* gene and (obviously) a hormonal stimulus as a second hit. Particularly in tumors with self-limited growth potential, endocrine stimulation might be a so far underestimated oncogenic driver.

ACKNOWLEDGMENTS

The authors thank the RNOH Research and Development Department and the RNOH Biobank Team for their support.

REFERENCES

1. Misiorowski W, Czajka-Oraniec I, Kochman M, et al. Osteitis fibrosa cystica-a forgotten radiological feature of primary hyperparathyroidism. *Endocrine*. 2017;58:380–385.
2. Nair PP, Gharote HP, Thomas S, et al. Brown tumor of the jaw. *BMJ Case Rep*. 2011;2011:bcr0720114465.
3. Sia H-K, Hsieh M-C, Yang L-H, et al. Maxillary brown tumor as initial presentation of parathyroid adenoma: a case report. *Kaohsiung J Med Sci*. 2012;28:400–403.
4. Xie C, Tsakok M, Taylor N, et al. Imaging of brown tumors: a pictorial review. *Insights Imaging*. 2019;10:75.
5. Dos Santos B, Koth VS, Figueiredo MA, et al. Brown tumor of the jaws as a manifestation of tertiary hyperparathyroidism: a literature review and case report. *Spec Care Dent*. 2018;38:163–171.
6. Gomes CC, Gayden T, Bajic A, et al. TRPV4 and KRAS and FGFR1 gain-of-function mutations drive giant cell lesions of the jaw. *Nat Commun*. 2018;9:4572.
7. Baumhoer D, Kovac M, Sperveslage J, et al. Activating mutations in the MAP-kinase pathway define non-ossifying fibroma of bone. *J Pathol*. 2019;248:116–122.
8. Schwarz C, Sulzbacher I, Oberbauer R. Diagnosis of renal osteodystrophy. *Eur J Clin Invest*. 2006;36(suppl 2):13–22.
9. Bovée JV, Hogendoorn PC. Non-ossifying fibroma: A RAS-MAPK driven benign bone neoplasm. *J Pathol*. 2019;248:127–130.
10. Guimarães LM, Gomes IP, Pereira TDSF, et al. KRAS mutations in brown tumor of the jaws in hyperparathyroidism. *J Oral Pathol*. 2020;49:796–802.
11. Guo S-W. Cancer driver mutations in endometriosis: variations on the major theme of fibrogenesis. *Reprod Med Biol*. 2018;17:369–397.
12. Buscail L, Bournet B, Cordelier P. Role of oncogenic KRAS in the diagnosis, prognosis and treatment of pancreatic cancer. *Nat Rev Gastroenterol Hepatol*. 2020;17:153–168.
13. Fernández-Medarde A, Santos E. Ras in cancer and developmental diseases. *Genes Cancer*. 2011;2:344–358.
14. Nikolaev SI, Vetiska S, Bonilla X, et al. Somatic activating KRAS mutations in arteriovenous malformations of the brain. *N Engl J Med*. 2018;378:250–261.
15. Anglesio MS, Papadopoulos N, Ayhan A, et al. Cancer-associated mutations in endometriosis without cancer. *N Engl J Med*. 2017;376:1835–1848.
16. Lac V, Nazeran TM, Tessier-Cloutier B, et al. Oncogenic mutations in histologically normal endometrium: the new normal? *J Pathol*. 2019;249:173–181.
17. Kato S, Lippman SM, Flaherty KT, et al. The Conundrum of genetic "drivers" in benign conditions. *J Natl Cancer Inst*. 2016;108:djw036.
18. Alberts B, Johnson A, Lewis J, et al. *Molecular Biology of the Cell*. New York, NY: Garland Science; 2002.
19. WHO Classification of Tumors Editorial Board. *WHO Classification of Tumors, Volume 3: Soft Tissue and Bone Tumors*, 5th ed. Lyon, France: International Agency for Research on Cancer; 2020.
20. Risques RA, Kennedy SR. Aging and the rise of somatic cancer-associated mutations in normal tissues. *PLoS Genet*. 2018;14:e1007108.
21. Kuznetsov SA, Cherman N, Riminucci M, et al. Age-dependent demise of GNAS-mutated skeletal stem cells and "normalization" of fibrous dysplasia of bone. *J Bone Miner Res*. 2008;23:1731–1740.